A EMPIRICAL MOTIVATION: USER BEHAVIORAL HETEROGENEITY

This appendix supplements Section 1 by quantifying *how much* of order-outcome variance is governed by stable user-level traits that are invisible to structured per-order features, motivating profiling as a complementary information source. All analyses use 38 days of City A production logs (44.3M dispatching records, 333,166 passengers, 12,128 active drivers).

Structured features leave large unexplained behavioral variance. We partition grabbed orders into 100 buckets defined by (fee quintile × ETA quintile × time-of-day), so orders within a bucket share nearly identical structured features. Within these matched buckets the PCR still varies substantially across users: the average within-bucket standard deviation is **24.9%**, and the P90–P10 spread reaches **37.1 percentage points**. A variance-component (ICC) analysis on the 31,160 passengers with ≥ 20 orders attributes **15.8%** of PCR variance to passenger identity alone: a stable, systematic signal that per-order features cannot expose.

Driver and passenger decile gaps under matched contexts. Figure 7 reports complementary cuts of the data. Panel (a) compares the most- vs. least-cancellation-prone passengers among those with ≥ 5 grabbed orders: despite virtually identical average order fee (19.8 vs. 19.0) and ETA (293s vs. 292s), the former's PCR reaches 32.6% while the latter's is 0.0%, a 32.6 p.p. gap. Panel (b) plots DAR percentiles across the 12,128 active drivers; the P90/P10 ratio is **8.2**× with $\sigma = 12.2\%$, far beyond what order-level features can account for. Panel (c) shows that driver cancellation behavior is similarly bimodal: top-decile DCR (38.1%) is **10.8**× the bottom decile (3.5%) under matched order conditions. Panel (d) quantifies the same effect at dispatching-round granularity: in 16.3% of 11.8M dispatching rounds (1.93M rounds) the same broadcasted order receives mixed outcomes from different drivers (some accept, others reject), and an extreme observed case had 18 of 19 drivers reject a single order with fee 17 and ETA 384s. These patterns are stable individual traits that profiling is designed to capture.

Heterogeneity is largely orthogonal to order-level features. Beyond decile-level summaries, we observe systematic individual preferences such as ETA-sensitivity heterogeneity (9.0% of 42,865 multi-ETA passengers exhibit >30 p.p. PCR swings across ETA bins; one passenger with 50 orders has 0% PCR at ETA 4–6 min but 100% at ETA >8 min) and driver price-tier selectivity (11.3% of 10,687 multi-tier drivers show ≥20 p.p. DAR gap between high- and low-price tiers, with a smaller 7.1% group exhibiting the opposite preference). The pilot study in Section 1 confirms that LLM-generated profiles convert these heterogeneity signals into 3.71% and 9.64% relative AUC gains on driver and passenger cancellation respectively, on top of a mature structured-feature predictor. Together, these analyses establish that user-side variance is large, systematic, and complementary to per-order features, precisely the gap ProfiLLM is designed to close.

Long-tail prevalence amplifies the need for clustering. Of the 333,166 unique passengers in the analysis window, **44.9%** appear in ≤ 3 orders and **59.3%** in ≤ 5 orders (consistent with Figure 2). For these users no individual-level behavioral signal can be reliably estimated,

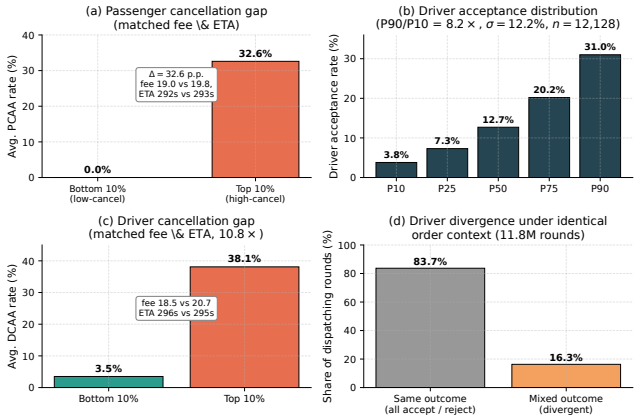

Figure 7: Behavioral heterogeneity invisible to structured features. (a) Passenger PCR decile gap under matched fee/ETA. (b) Driver DAR percentiles. (c) Driver DCR decile gap under matched conditions. (d) Share of dispatching rounds in which the same broadcasted order receives divergent accept/reject decisions from different drivers.

motivating ProfiLLM's adaptive cluster-level profiling that transfers knowledge from data-rich groups to data-sparse individuals.

B REPRESENTATIVE CASE STUDIES

To illustrate the kind of behavioral heterogeneity that ProfiLLM's profile embeddings are designed to capture, we walk through two representative cases drawn from City A production logs.

Driver case: divergent acceptance under nearly identical order context. In a single dispatching round, order `2209******7356` (fee \$17.0, ETA 384 s, evening hour 17, origin/destination both in the city center) was broadcast to **19 drivers**. Only **one driver accepted**; the other **18 rejected**. The accepting driver had a baseline DAR of 0.089 and historical completion rate of 0.289; a representative rejecting driver had DAR 0.114 and completion rate 0.222, so a predictor relying purely on order-side and aggregate driver-side structured statistics would have ranked the rejecting driver *higher*. Across the full log, **16.3%** of dispatching rounds (1.93 M of 11.8 M batches) exhibit such mixed-outcome broadcasts where the same order receives divergent accept/reject decisions from different drivers under near-identical order-side context (Appendix A). ProfiLLM's cluster-level driver profile encodes precisely this kind of identity-driven pattern, e.g., the accepting driver's cluster is characterized by a willingness to take evening city-center orders with mid-tier fares, while the rejecting drivers' clusters are not.

Passenger case: ETA-sensitivity stratification under matched fare. The most cancellation-prone passengers in City A (18,394 passengers, average PCR 32.6%) book at average fare \$19.8 and ETA 293 s; a comparison group of 97,579 passengers exhibits PCR 0.0% under almost identical conditions (fare \$19.0, ETA 292 s). A finer-grained example: passenger `8796******8501` (50 grabbed orders) cancels **0%** of orders with ETA in 4–6 min but **100%** of orders with ETA > 8 min, while the platform average rises only from 6.9% to 11.3% across

the same ETA band. This per-passenger ETA-tolerance threshold is invisible to structured features that report only the absolute ETA value; ProfiLLM's cluster-level passenger profile materializes such latent tolerance patterns as part of the cluster's PROFILE narrative (e.g., "commute-hour passengers who tolerate ≤ 6 min wait but defect at longer ETAs"), feeding the prediction model a discriminative signal the structured-feature baseline cannot express.

C BACKGROUND

Tool-Augmented LLM Agents. Recent advances have demonstrated that LLMs can effectively leverage external tools to accomplish complex tasks beyond their inherent capabilities [13, 22, 26, 37, 45]. A tool-augmented LLM agent operates by iteratively generating reasoning traces and invoking tools based on intermediate observations. Formally, given an input query q and a tool set $\mathcal{T} = \{t_1, \ldots, t_{|\mathcal{T}|}\}$, the agent produces a trajectory $\tau = \{(a_i, r_i)\}_{i=1}^{L}$, where a_i denotes an action (either reasoning or tool invocation) and r_i denotes the corresponding observation or tool result. This paradigm enables LLMs to analyze data at scales far exceeding their context window limitations.

Direct Preference Optimization (DPO). DPO [28] provides an efficient approach to align LLM outputs with human preferences without explicit reward modeling. Given preference pairs (x, y_w, y_l) where y_w is preferred over y_l for input x, DPO directly optimizes the policy π_θ via:

$$\mathcal{L}_{\text{DPO}} = -\mathbb{E}_{(x,y_w,y_l)}\left[\log \sigma\left(\beta \log \frac{\pi_\theta(y_w|x)}{\pi_{\text{ref}}(y_w|x)} - \beta \log \frac{\pi_\theta(y_l|x)}{\pi_{\text{ref}}(y_l|x)}\right)\right] \tag{7}$$

where π_{ref} is a reference policy (typically the supervised fine-tuned model), β controls the deviation from the reference, and $\sigma(\cdot)$ is the sigmoid function. In our context, we extend DPO to align profile generation with downstream prediction utility.

D ANALYTICAL TOOL DETAILS

Table 4 presents the complete categorization of the 27 analytical tools used in the Tool-Augmented Global Knowledge Mining module. These tools are organized into six categories based on their analytical functionality: (1) **Statistical** tools for computing aggregate statistics, comparing segments, clustering users, and identifying important features; (2) **Causal** tools for discovering causal relationships, performing counterfactual analysis, and conducting multi-stage iterative mining with uncertainty quantification; (3) **Knowledge** tools for extracting global causal rules, generating classification benchmarks, and constructing profile knowledge bases; (4) **Validation** tools for verifying discovered patterns and cross-validating conclusions; (5) **Spatiotemporal** tools for detecting peak periods, analyzing day-of-week and hourly patterns, identifying spatial hotspots, and examining origin-destination flows; and (6) **Contextual** tools for analyzing supply-demand balance, wait time factors, matching efficiency, anomalies, special periods, and weather impacts. All tools are designed to accept structured parameters and return interpretable results that the LLM agent can reason over, enabling composable tool chains for complex analytical queries.

Algorithm 1 Tool-Augmented Global Knowledge Mining

Require: Historical data $\mathcal{H}$, Tool set $\mathcal{T}$, LLM agent $\mathcal{M}$
Ensure: Global knowledge $\mathcal{K}$, Clustering rules $\mathcal{A}$, Regional priors $\mathcal{R}$

// Phase 1: Explore
$findings_1 \leftarrow \emptyset$
for $t \in \mathcal{T}_{basic}$ **do**
  $result \leftarrow t$.execute($\mathcal{H}$)
  $findings_1 \leftarrow findings_1 \cup \mathcal{M}$.interpret($result$)
end for
// Phase 2: Deepen
$directions \leftarrow \mathcal{M}$.identify_directions($findings_1$)
$findings_2 \leftarrow \emptyset$
for $dir \in directions$ **do**
  $tools \leftarrow \mathcal{M}$.select_tools($dir, \mathcal{T}$)
  $result \leftarrow$ ExecuteToolChain($tools, \mathcal{H}$)
  $findings_2 \leftarrow findings_2 \cup \mathcal{M}$.analyze($result$)
end for
// Phase 3: Validate
$candidates \leftarrow \mathcal{M}$.extract_hypotheses($findings_1 \cup findings_2$)
$validated \leftarrow \emptyset$
for $hyp \in candidates$ **do**
  $pval, eff \leftarrow$ `validate_hypothesis`($hyp, \mathcal{H}$)
  if $pval < \alpha$ **and** $|eff| > \epsilon$ **then**
    $validated \leftarrow validated \cup \{(hyp, eff)\}$
  end if
end for
// Phase 4: Synthesize
$\mathcal{K} \leftarrow \mathcal{M}$.synthesize_knowledge($validated$)
$\mathcal{A} \leftarrow \mathcal{M}$.generate_clustering_rules($findings_2$)
$\mathcal{R} \leftarrow$ `compute_regional_priors`($\mathcal{H}, \mathcal{G}$)
return $\mathcal{K}, \mathcal{A}, \mathcal{R}$

E ALGORITHM PSEUDOCODE

This section provides the detailed pseudocode for the two core procedures in ProfiLLM.

Algorithm 1 formalizes the Tool-Augmented Global Knowledge Mining workflow described in Section 3.2. The procedure follows the four-phase Explore-Deepen-Validate-Synthesize paradigm. In the Explore phase, the agent invokes basic statistical tools to obtain an initial understanding of the data landscape. The Deepen phase identifies promising analytical directions from preliminary findings and applies targeted tool chains for focused investigation. The Validate phase subjects each discovered pattern to statistical hypothesis testing, retaining only findings with p-value below threshold α and effect size exceeding ϵ. Finally, the Synthesize phase consolidates validated findings into three structured outputs: global knowledge $\mathcal{K}$, user clustering rules $\mathcal{A}$, and regional supply-demand priors $\mathcal{R}$.

Algorithm 2 details the DPO-Aligned Profile Exploration procedure described in Section 3.3. Given a user cluster a with its aggregated history and the global knowledge base, the algorithm first generates K diverse candidate profiles and evaluates each via the LOGIC-rule-based utility proxy (Eq. 4). The best-performing candidate then undergoes iterative refinement for T rounds: at each iteration, prediction errors are analyzed to produce targeted feedback, and the LLM generates an improved profile conditioned on this feedback. Throughout the process, all candidate profiles are compared pairwise to construct preference pairs with a margin threshold γ, which are subsequently used for DPO fine-tuning to

Table 4: Categorization of analytical tools in ProfiLLM.

Category	#	Tool	Description
Statistical	4	`AggregateStats`	Calculate aggregate statistics by dimension
		`CompareSegments`	Compare segments on specific metrics
		`UserClustering`	K-Means clustering on user behavior
		`FeatureImportance`	Analyze key features for target metric
Causal	5	`CausalDiscovery`	Discover causal relationships
		`CounterfactualAnalysis`	Perform "what if" analysis
		`ChainOfMining`	Multi-stage iterative analysis
		`UncertaintyAwareMining`	Provide confidence intervals
		`ContrastiveAnalysis`	Compare similar groups for differences
Knowledge	3	`GlobalCausalRules`	Discover global causal rules
		`GlobalBenchmarks`	Generate benchmarks for classification
		`ProfileKnowledgeBase`	Generate profile usage guide
Validation	2	`ValidationDiscovery`	Validate discovered patterns
		`ConclusionValidation`	Cross-validate conclusions
Spatio-temporal	6	`DetectPeakPeriods`	Detect peak periods for metrics
		`DayOfWeekPattern`	Analyze weekday vs weekend patterns
		`HourlyPattern`	Analyze 24-hour detailed patterns
		`SpatialHotspot`	Identify spatial distribution hotspots
		`ODFlowAnalysis`	Analyze origin-destination flow patterns
		`RegionCharacteristics`	Analyze regional characteristic profiles
Contextual	7	`SupplyDemandAnalysis`	Analyze supply-demand balance
		`WaitTimeFactors`	Analyze factors affecting wait time
		`MatchingEfficiency`	Analyze order matching efficiency
		`DetectAnomalies`	Detect anomalies in metrics
		`SpecialPeriodAnalysis`	Analyze holiday/event patterns
		`WeatherFactorAnalysis`	Analyze weather impact on metrics
		`WeatherScenario`	Analyze specific weather scenarios

align the LLM's generation capability with downstream prediction utility.

Algorithm 2 Utility-Aligned Profile Exploration

Require: Cluster a, Aggregated history $\mathcal{H}_a$, Global knowledge $\mathcal{K}$, LLM $\mathcal{M}$
Ensure: Optimal profile $profile_a^*$, Preference pairs $\mathcal{P}_a$

// *Initial candidate generation*
$\{profile_a^{(k)}\}_{k=1}^{K} \leftarrow \mathcal{M}.\text{generate}(\mathcal{H}_a, \mathcal{K}, K)$
// *Evaluate initial candidates via LOGIC rules*
for $k = 1$ **to** K **do**
  $LOGIC_a^{(k)} \leftarrow \text{extract\_logic}(profile_a^{(k)})$
  $\Delta_a^{(k)} \leftarrow \text{EvaluateUtility}(LOGIC_a^{(k)}, \mathcal{H}_a)$ ▷ Eq. 4
end for
$k^* \leftarrow \arg\max_k \Delta_a^{(k)}$
$profile_a^{best} \leftarrow profile_a^{(k^*)}$; $\Delta_a^{best} \leftarrow \Delta_a^{(k^*)}$
// *Iterative refinement*
for $t = 1$ **to** T **do**
  $feedback \leftarrow \text{AnalyzeErrors}(LOGIC_a^{best}, \mathcal{H}_a)$
  $\{profile_a^{(t,k)}\}_{k=1}^{K} \leftarrow \mathcal{M}.\text{refine}(profile_a^{best}, feedback, K)$
  for $k = 1$ **to** K **do**
    $\Delta_a^{(t,k)} \leftarrow \text{EvaluateUtility}(profile_a^{(t,k)}, \mathcal{H}_a)$
  end for
  $k^\dagger \leftarrow \arg\max_k \Delta_a^{(t,k)}$
  if $\Delta_a^{(t,k^\dagger)} > \Delta_a^{best}$ **then**
    $profile_a^{best} \leftarrow profile_a^{(t,k^\dagger)}$; $\Delta_a^{best} \leftarrow \Delta_a^{(t,k^\dagger)}$
  end if
end for
$profile_a^* \leftarrow profile_a^{best}$
// *Construct preference pairs for DPO*
$\mathcal{P}_a \leftarrow \{(\mathcal{H}_a, profile_w, profile_l) : \Delta_w > \Delta_l + \gamma\}$
return $profile_a^*$, $\mathcal{P}_a$

F DISCOVERED CLUSTER ARCHETYPES

ProfiLLM's clustering rules are *not* manually specified. They are produced by the LLM agent during the Synthesize phase of Tool-Augmented Global Knowledge Mining (Algorithm 1), which interprets cluster centroids and their z-score deviations from the population mean to assign meaningful archetype labels. Drivers and passengers are clustered separately into $A = A_D \cup A_P$, where the agent settled on $|A_D| = 28$ driver clusters and $|A_P| = 49$ passenger clusters in our main experiments. Clustering uses dozens of behavioral features, including order volume and frequency, acceptance/grab rate, cancellation rate and patterns, completion rate, average fee and price sensitivity, active-time distribution, trip distance and duration, spatial activity patterns, and derived ratios (e.g., cancel-to-complete ratio, peak-hour share).

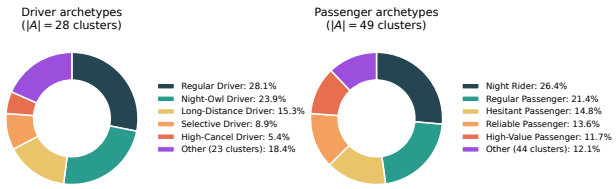

Figure 8: Population share of the top-5 LLM-discovered archetypes in City A for drivers ($|A_D| = 28$) and passengers ($|A_P| = 49$), with the remaining clusters aggregated for clarity.

Figure 8 reports the population share of the top-5 archetypes for each role, and Table 5 lists their defining characteristics. The dominant driver groups (Regular, Night-Owl, Long-Distance, Selective, High-Cancel) together cover 81.6% of the active driver fleet, while the corresponding top-5 passenger groups cover 87.9% of the passenger population. Tail clusters retain meaningful distinctions (e.g., airport-specialist drivers, time-sensitive commuter passengers) that the LLM agent labels using domain-grounded heuristics from the mined global knowledge.

F.1 User Cluster Embedding Visualization

To qualitatively assess whether the clustering rules $\mathcal{A}$ yield behaviorally separable groups, we visualize user-level embedding distributions via t-SNE [21]. For each user $u \in \mathcal{P} \cup \mathcal{D}$, we extract a behavioral feature vector from $\mathcal{H}_u$ and assign them to cluster $a^*(u)$ via rules $\mathcal{A}$. Before dimensionality reduction, we apply core filtering (retaining the nearest 80% of points to each cluster centroid) and stratified sampling (capping at 15,000 points per role). The filtered embeddings are standardized, reduced to 50 dimensions via PCA,

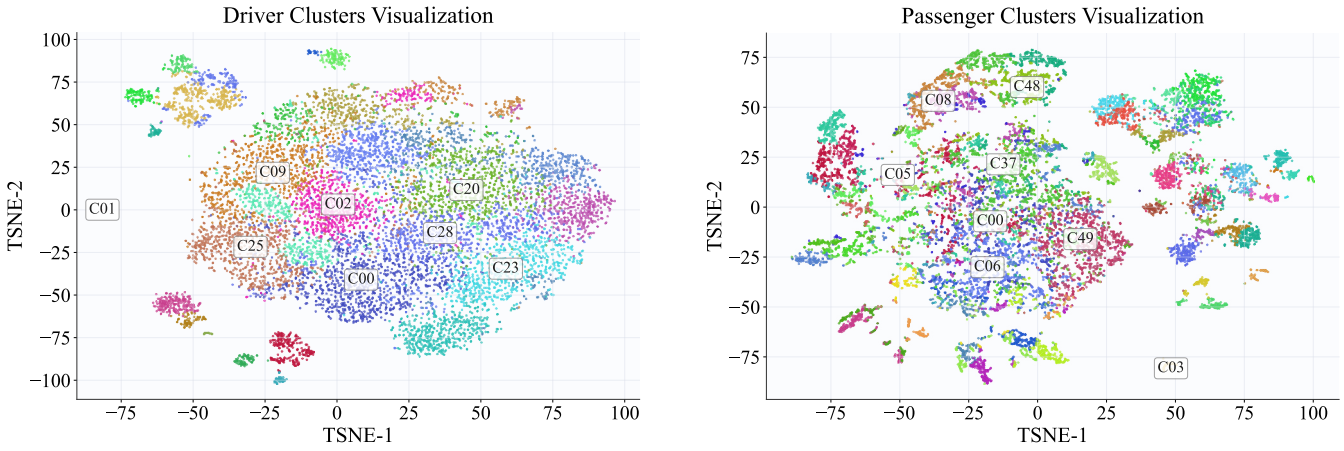

(a) Driver clusters

(b) Passenger clusters

Figure 9: t-SNE visualization of user cluster embeddings in City A, showing (a) driver clusters and (b) passenger clusters. Each point represents a user colored by cluster assignment; the top-8 largest clusters are labeled at their median positions.

Table 5: Representative archetypes discovered by the LLM agent in City A. Listed signatures are cluster-centroid characteristic values (salient deviations from the population mean) used by the agent for labeling, not realized post-acceptance PCR/DCR rates.

Archetype	Share	Key behavioral signatures
Driver		
Regular Driver	28.1%	Moderate activity, morning-dominant hours
Night-Owl Driver	23.9%	Avg. hour 16.1, high evening concentration
Long-Distance Driver	15.3%	Avg. fee 20.8, avg. trip 7.7 km
Selective Driver	8.9%	Low volume but 44.6% grab rate
High-Cancellation Driver	5.4%	Cancel rate 84.5%, low completion
Passenger		
Night Rider	26.4%	Avg. hour 16.8, evening-dominant
Regular Passenger	21.4%	Moderate volume, morning-focused
Hesitant Passenger	14.8%	Cancel rate 69.6%, low reliability
Reliable Passenger	13.6%	Low volume, completion rate 46.9%
High-Value Passenger	11.7%	Avg. fare 34.0, avg. trip 14.1 km

and projected to 2D with t-SNE (perplexity = 35, PCA initialization, seed = 42).

Figure 9 presents the resulting scatter plots for City A, with the top-8 largest clusters annotated at their median positions. The driver embedding space (Figure 9 (a)) exhibits well-separated clusters corresponding to discovered archetypes, including *Regular Drivers* (C00), *Night Owls* (C01), and *Long-Distance Drivers* (C02). The passenger embedding space (Figure 9 (b)) similarly reveals distinct groups such as *Night Riders*, *Regular Passengers*, and *Hesitant Passengers* with elevated cancellation tendencies, though with more overlap reflecting higher behavioral diversity on the passenger side. The clear visual separation confirms that the LLM-agent-derived clustering rules partition users into behaviorally coherent groups, supporting cluster-level profiles as effective proxies for individual user behavior in downstream outcome prediction.

G DISPATCHING SIMULATOR ARCHITECTURE

We summarize the design choices that make our simulator a faithful and reproducible offline counterpart to production dispatcher.

Replay-based discrete-event environment. The simulator replays five full days of historical order arrivals and driver availability per city, rather than generating synthetic demand. All orders arrive at their actual timestamps with real origin, destination, dynamic pricing (including surge multipliers), and over 30 contextual features. Driver positions are initialized from actual GPS trajectory logs, and each driver's online-duration distribution is reconstructed from historical records. The geographic space uses the same production grid system, preserving real-world spatiotemporal distributions of demand, supply, and traffic.

Production-identical dispatching cadence and matching. The simulator operates in 2-second dispatching cycles. At each cycle, candidate OD pairs are enumerated within a 1,500-meter pickup radius; the production STR (Spatio-Temporal Revenue) formula scores each pair using Accept/P-Cancel/D-Cancel predictions, pickup cost, and order value with production-calibrated weights; and the optimal bipartite assignment is solved via a Lagrangian-relaxation variant of Kuhn–Munkres, identical to the algorithm deployed in production.

Production routing API integration. The simulator queries DiDi's production routing service via Thrift RPC to obtain live-traffic-aware ETA and pickup distance (with 25th/75th-percentile confidence intervals), eliminating a major source of bias that approximate offline routing would introduce.

Three-stage stochastic outcome simulation. Rather than sampling a single completion probability, the simulator implements a three-stage sequential decision process: (i) Accept sampling (driver acceptance); (ii) conditional D-Cancel sampling; (iii) P-Cancel sampling. An order completes *only if* the driver accepts and neither party

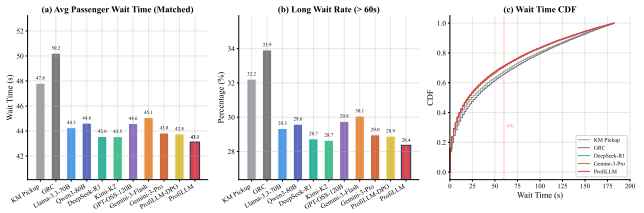

Figure 10: Passenger wait time analysis in the dispatching simulator. (a) Average wait time for matched orders. (b) Proportion of orders with wait time exceeding 60 seconds. (c) Cumulative distribution function (CDF) of wait times for representative strategies.

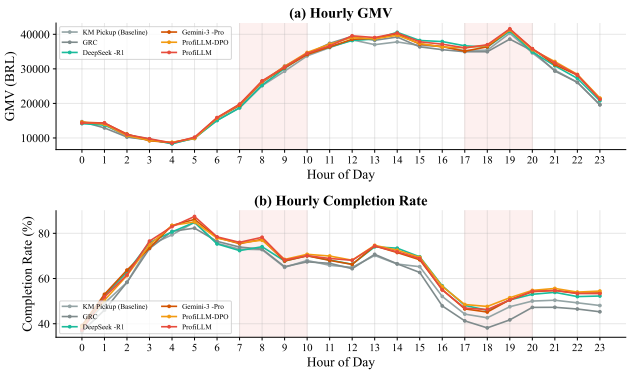

Figure 11: Hourly GMV and CR in the dispatching simulator. Shaded regions indicate peak hours (morning 7–10, noon 11–14, evening 17–20).

cancels. Failed orders re-enter the pending queue for re-dispatch up to a 180-second patience timeout, producing realistic re-dispatch cascades. This three-stage design captures the feedback loop in which a better predictor yields better matches, fewer rejections, fewer re-dispatches, and higher system-wide efficiency.

Dynamic state evolution. Drivers transition between *idle*, *en-route-to-pickup*, and *in-service* states with real-time features refreshed every cycle, ensuring that downstream feature distributions remain consistent with production. Orders follow realistic lifecycle transitions with timeouts, and grid-level supply-demand statistics support spatial-aware matching weights.

Validation against production. Comparing simulation (Table 1, City A) with the 14-day online A/B test (Figure 5) shows directional consistency on every core metric (GMV, CR, PCR, DCR all moving in the desired direction), though the online deltas are several times smaller (*e.g.,* **+0.47%** vs. **+4.02%** GMV, a ∼8–9× gap). Simulation magnitudes exceed online deltas because the simulator both scores candidate matches and samples their outcomes from the *same* model, grading each policy on its own beliefs in a closed loop that omits the live confounders (driver multi-homing, exogenous demand shocks, concurrent experiments) which attenuate real treatment effects; this downward bias is well documented for two-sided-marketplace experiments [10]. This direction-preserving, magnitude-inflating behavior is characteristic of replay-based ride-hailing simulators [27, 42, 44] and mirrors the broader offline-to-online gap, in which offline metrics overstate online performance while better preserving method ranking [9]. The key validation criterion is therefore directional consistency and method ranking preservation, both of which our simulator delivers.

H PASSENGER WAIT TIME ANALYSIS

We further analyze passenger wait time in the dispatching simulator to evaluate user experience beyond platform-level metrics. As shown in Figure 10, the two non-LLM baselines exhibit the highest average wait times (GRC: 50.2s, KM Pickup: 47.8s), while all LLM-based strategies achieve notably lower values ranging from 43.1s to 45.1s. ProfiLLM attains the lowest average wait time of 43.1s, representing reductions of 9.8% over KM Pickup and 14.1% over GRC. The long-wait rate (>60s) follows a consistent pattern: GRC and KM Pickup reach 33.9% and 32.2%, respectively, whereas ProfiLLM reduces this to 28.4%. The CDF curves further confirm a systematic leftward shift for ProfiLLM across all quantiles, indicating that the improvement is not driven by a small subset of orders but reflects enhanced dispatching efficiency throughout. These results complement the GMV and CR metrics in Section 4.2, demonstrating that utility-aligned user profiles improve not only platform revenue but also passenger-perceived service quality.

I HOURLY PERFORMANCE ANALYSIS

To understand how different strategies perform across varying demand conditions, we analyze hourly GMV and CR in the dispatching simulator. As shown in Figure 11, all strategies follow the same demand pattern with peaks around noon (12–13h) and evening (18–19h), and a trough in the early morning (4–5h). ProfiLLM and ProfiLLM-DPO consistently outperform baselines throughout the day, with the gap most pronounced during evening peak hours (17–20h) when supply-demand imbalance intensifies and accurate outcome prediction becomes critical. Notably, GRC suffers a sharp CR drop during evening hours (falling below 40%), likely due to its cooperative game formulation struggling under severe supply constraints, whereas ProfiLLM maintains stable performance above 50%. The consistent hourly advantage confirms that utility-aligned user profiles provide robust improvements across diverse operational conditions rather than benefiting only specific time periods.

J CLUSTER-COUNT SENSITIVITY

To verify that the framework is robust to the granularity of clustering, we evaluate 11 cluster configurations on City A by varying one side while fixing the other: $|A_D| \in \{8, 16, 32, 64, 128, 256\}$ at $|A_P| = 64$, and $|A_P| \in \{8, 16, 32, 64, 128, 256\}$ at $|A_D| = 32$. Each configuration is evaluated against 9 LLM backbones (the 7 baselines in Table 2 plus ProfiLLM and ProfiLLM-DPO), totaling 99 runs.

Figure 12 shows that both ProfiLLM and ProfiLLM-DPO produce stable AUC across the entire sweep. Performance climbs from 8 to 16 clusters per side and then plateaus, with variation within 0.6 p.p. absolute AUC for all four tasks. Across all 11 cluster configurations, both ProfiLLM and ProfiLLM-DPO outperform the structured-only baseline on Accept, D-Cancel, and P-Cancel at every cluster count; among the 99 runs the un-aligned baseline backbones remain mixed

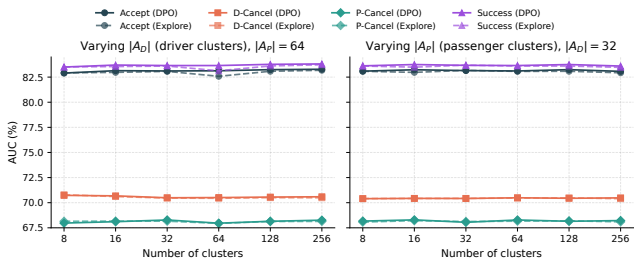

Figure 12: Cluster-count sensitivity for ProfiLLM (dashed) and ProfiLLM-DPO (solid) on City A, with each curve aggregated over 9 LLM backbones. Left: varying $|A_D|$ with $|A_P| = 64$. Right: varying $|A_P|$ with $|A_D| = 32$. The cross-model standard deviation across the 9 backbones is 0.05%–0.27%.

(consistent with Table 2), confirming that the ProfiLLM gains observed in the main paper are not specific to a particular cluster count. Across the same sweep, the two variants are statistically indistinguishable on prediction AUC: average $\Delta = +0.14\%$ (Accept), +0.05% (D-Cancel), +0.02% (P-Cancel), and +0.14% (Success), with the sign of Δ fluctuating across configurations rather than systematically favoring either variant. This supports our deployment choice of ProfiLLM-DPO, which achieves comparable prediction quality at substantially lower offline refresh cost (Appendix M).

K UTILITY-PROXY SENSITIVITY TO THE BLENDING COEFFICIENT λ

The blending coefficient λ in Eq. (3) controls how strongly the LOGIC rules are mixed with the base production model during *offline profile evaluation*. It does not appear in the online prediction model. We perform a grid search over $\lambda \in \{0, 0.1, \ldots, 1.0\}$ across 6 cluster granularities for each of 3 outcome tasks, yielding 494 cluster-task combinations (21 driver-accept, 82 driver-cancel, 391 passenger-cancel clusters; counts vary because clusters with insufficient behavioral data are filtered out).

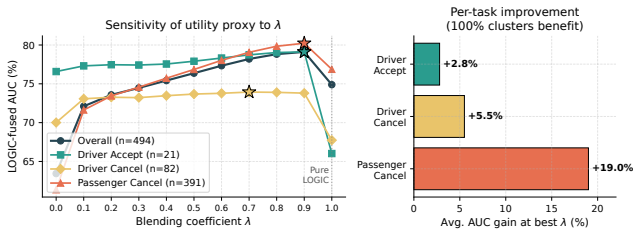

Figure 13: Sensitivity of the LOGIC-rule utility proxy to the blending coefficient λ. Left: per-task LOGIC-fused AUC versus $\lambda \in [0, 1]$, averaged across 494 cluster-task combinations; stars mark each task's peak. Right: average AUC gain at the best λ for each task. $\lambda = 1.0$ denotes pure LOGIC with the base model discarded.

Figure 13 (left) reports the average LOGIC-fused AUC as a function of λ. Three patterns are clear: (1) All tasks improve over $\lambda = 0$ (base model only) once blending is introduced, demonstrating that LOGIC rules supply *complementary* discriminative signal beyond structured features. (2) All tasks collapse at $\lambda = 1.0$ (pure LOGIC, base model discarded), confirming the conservative design that retains the strong production predictor. (3) The optimum is task-dependent: Driver Accept and Passenger Cancel peak at $\lambda = 0.9$, whereas Driver Cancel peaks at $\lambda = 0.7$–0.8 and stays remarkably flat over $\lambda \in [0.1, 0.9]$. At the cluster level, 65.7% of passenger clusters prefer $\lambda = 0.9$ while 40.2% of driver-cancel clusters prefer $\lambda = 0.1$, motivating adaptive per-cluster λ selection as a direction for future work.

Figure 13 (right) summarises the per-task gain at each task's best λ: +2.8% (Driver Accept), +5.5% (Driver Cancel), and +19.0% (Passenger Cancel). The cancellation tasks gain the most, mirroring the prediction-AUC pattern in Table 2: behavioral profiling shines exactly where structured features struggle most, namely in capturing the contextual decision logic behind cancellations.

L DPO VS. EXPLORATION: WHY BOTH VARIANTS HELP

A natural question is why we report both ProfiLLM (exploration only) and ProfiLLM-DPO (with DPO fine-tuning) when their per-task prediction AUCs in Table 2 are similar. The two variants are complementary by design, and we clarify their roles below.

(1) DPO targets generator efficiency, not per-task AUC.. ProfiLLM (exploration) generates $K = 5$ candidate profiles per cluster and refines the best for $T = 3$ iterations. The theoretical upper bound is $K(1 + T) = 20$ LLM calls per cluster (5 initial + 5 re-explored per refinement iteration), which we cap at 15 in deployment for compute efficiency. ProfiLLM-DPO generates a high-quality profile in a *single pass*, eliminating the iterative search. When profiles are refreshed for new clusters, new cities, or updated behavioral data, this collapses the offline LLM-call budget by an order of magnitude (Appendix M). Both variants serve identically online via cached embeddings; the difference is purely offline.

(2) The two variants achieve comparable prediction quality across configurations. Across the 11 cluster configurations of Appendix J, the average inter-variant gap is only +0.14% (Accept AUC), +0.02% (P-Cancel AUC), and +0.14% (Success AUC), with the sign of the gap fluctuating across configurations rather than systematically favoring either variant (maximum absolute deviation is 0.55 p.p.). Both variants substantially outperform all 7 baseline LLMs in every metric and every city (Tables 1–2), so the choice between them is dominated by cost, not quality.

(3) Per-task differences in Table 2 reflect different optimization strategies, not degradation. ProfiLLM (exploration) performs *per-cluster local optimization*: it iteratively searches profile space for each cluster, and the LOGIC-rule AUC proxy directly drives the selection. ProfiLLM-DPO aggregates preference pairs *across clusters* and learns a single generator (Qwen3-8B) that produces high-utility profiles in one pass. The latter trades a small amount of per-cluster local optimality for cross-cluster generalization. A second, subtler factor is the *signal-channel gap*: DPO is supervised on LOGIC-rule AUC (a discrete Boolean projection), while the downstream prediction model consumes PROFILE *text embeddings* (continuous dense vectors). The two share the same behavioral understanding but

are not identical, so DPO optimization on one does not transfer perfectly to the other. Finally, online GMV is a composite matching objective over all three predicted outcomes, so small per-task differences can cancel or compound through the matching weights.

We therefore deploy ProfiLLM-DPO in production because it achieves comparable prediction quality at substantially lower offline refresh cost, enabling faster iteration when scaling to new clusters and cities.

M OFFLINE SYSTEM COST ANALYSIS

Table 6 reports the end-to-end offline cost of running ProfiLLM on a single city with $|A_D| = 32$ driver clusters and $|A_P| = 64$ passenger clusters using Gemini-3-Pro as the analyst LLM (input \$1.25/1M tokens, output \$10.00/1M tokens). Downstream model training uses one NVIDIA L20 GPU (48GB) at \$1.50/GPU-hour.

Table 6: Offline pipeline cost breakdown for one city. The Profile + Exploration LLM-call count is $(32 + 64) \times 15 = 1{,}440$, where 15 is the deployed per-cluster cap (theoretical max $K(1 + T) = 20$ with $K = 5, T = 3$).

Stage	Hardware	Wall Time	LLM Calls	Tokens (in/out)	Cost
Initial run (ProfiLLM, exploration)					
Global Knowledge Mining	CPU+API	∼50 min	∼20	2M/0.5M	\$7.50
Profile + Exploration	CPU+API	∼240 min	∼1,440	12M/3M	\$45.00
Downstream Training	1×L20	∼85 min	0	–	\$2.13
Total initial	–	**∼6.3 hrs**	**∼1,460**	14M/3.5M	**\$54.63**
Subsequent refresh (ProfiLLM-DPO, single-pass)					
Profile Generation	CPU+API	∼25 min	96	0.8M/0.2M	\$3.00
Downstream Training	1×L20	∼85 min	0	–	\$2.13
Total refresh	–	**∼1.8 hrs**	**96**	0.8M/0.2M	**\$5.13**

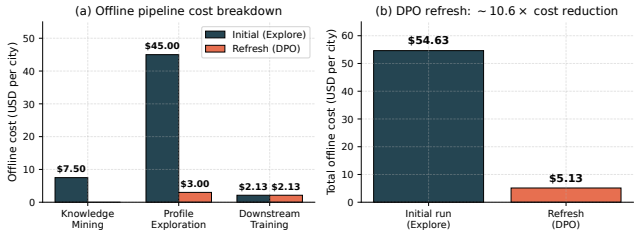

Figure 14: Offline cost breakdown. (a) Per-stage cost for the initial ProfiLLM run vs. a single-pass DPO refresh. (b) Total per-city offline cost for the two settings.

Three observations follow (Figure 14). (1) **Cluster-level profiling drives cost efficiency**: 96 cluster-level profiles cover all 348,464 users in City A, a 3,630× reduction over per-user profiling and the precondition for affordable LLM-driven profiling at platform scale. (2) **DPO compounds the efficiency gain**: once DPO is trained, subsequent refreshes require only 96 single-pass calls, reducing per-city LLM cost from \$52.50 to \$3.00 and total refresh cost from \$54.63 to \$5.13 (∼ 10.6× reduction). (3) **Online overhead is negligible**: at serving time the system performs only deterministic cluster assignment (<0.01 ms) and a cached embedding lookup (<0.001 ms), well within DiDi's 200 ms latency budget; no LLM is queried online.

The 14-day A/B improvement of +0.47% GMV on a platform processing millions of daily orders translates into revenue gains that exceed the offline cost by several orders of magnitude, even before considering the platform-side savings from reduced cancellations and bad-experience rates.

N COMPLEXITY ANALYSIS

We analyze the computational complexity of ProfiLLM along offline, online, and storage dimensions, and compare against per-user profiling. Notation follows Section 2: $M = |\mathcal{P}|$ passengers and $N = |\mathcal{D}|$ drivers; $\mathcal{H} = \bigcup_u \mathcal{H}_u$ aggregated history with $|\mathcal{H}| = \sum_u |\mathcal{H}_u|$; $\mathcal{A} = \mathcal{A}_D \cup \mathcal{A}_P$ cluster set; K=5 candidates per generation, T=3 refinement iterations; d=768 embedding dimension; and $|C|$ candidate OD pairs per dispatching cycle.

N.1 Offline Complexity

(O1) Knowledge Mining (Algorithm 1). Each tool performs at most a single pass over $\mathcal{H}$ at $O(|\mathcal{H}|)$ cost. The Explore phase invokes the basic tool set $\mathcal{T}_{basic} \subset \mathcal{T}$; Deepen and Validate may then invoke any tool in $\mathcal{T}$ via targeted chains, with each tool used at most once across the workflow (so the total tool-invocation count is $O(|\mathcal{T}|)$). The aggregate tool-execution cost is therefore $O(|\mathcal{T}| \cdot |\mathcal{H}|)$. The LLM agent issues a constant number of reasoning calls (≈20 in deployment, Table 6), independent of $|\mathcal{H}|$. This stage is linear in data and constant in LLM calls.

(O2) Cluster Assignment. For each user u, we evaluate $|\mathcal{A}|$ membership rules over $\mathcal{H}_u$, costing $O(|\mathcal{A}| \cdot |\mathcal{H}_u|)$. Summed over all users this is $O(|\mathcal{A}| \cdot |\mathcal{H}|)$ and is embarrassingly parallel.

(O3) Profile Exploration (Algorithm 2). Per cluster a with aggregated history $\mathcal{H}_a$ (where $\sum_a |\mathcal{H}_a| \le |\mathcal{H}|$), the initial generation issues K LLM calls, and each of the T refinement iterations regenerates K candidates conditioned on prediction-error feedback, contributing KT additional calls; every generated candidate's LOGIC rule is then evaluated over $\mathcal{H}_a$ at $O(|\mathcal{H}_a|)$ cost. Aggregating over clusters:

$$\text{LLM calls} = O\big(|\mathcal{A}| \cdot K(1+T)\big), \qquad \text{LOGIC eval} = O\big(K(1+T) \cdot |\mathcal{H}|\big).$$

The theoretical upper bound is $K(1 + T) = 20$ calls per cluster; in deployment we cap total calls at 15 per cluster, which corresponds to early-terminating refinement after at most two iterations of the K-candidate regeneration, yielding $|\mathcal{A}| \cdot 15 = 1{,}440$ calls per city for $|\mathcal{A}| = 96$ (Table 6). This is the LLM-call-dominated stage, but the cost is amortized across all users in each cluster.

(O4) DPO Fine-tuning. Preference-pair construction over the $K(1 + T)$ profiles per cluster is at most $O\big(|\mathcal{A}| \cdot K^2(1 + T)^2\big)$. The DPO training cost is the standard LLM fine-tuning loop, $O(E \cdot |\mathcal{P}_{pref}| \cdot L \cdot c_{LLM})$, where E is the number of epochs, L is profile token length, and c_{LLM} denotes the per-token forward+backward FLOPs of the base model. In our deployment this takes ≈85 minutes on one NVIDIA L20 GPU.

(O5) Embedding Precomputation. A single encoder forward per cluster profile: $O(|\mathcal{A}| \cdot L \cdot c_{enc})$. Empirically negligible (seconds for $|\mathcal{A}|$=96).

N.2 Online Complexity (Per Dispatching Cycle)

(N1) Per OD-pair scoring. Passenger and driver cluster IDs are pre-assigned offline and refreshed at user registration; serving requires only two $O(1)$ cache lookups returning $\mathbf{e}_p, \mathbf{e}_d \in \mathbb{R}^d$, an $O(d)$ feature concatenation, and a constant-cost prediction-network forward $O(c_f)$.

(N2) Per-cycle cost. For $|C|$ candidate OD pairs the per-cycle cost is $O\big(|C| \cdot (d + c_f)\big) + O_{\mathrm{KM}}(|C|)$, where O_{KM} denotes the production Lagrangian-relaxation Kuhn–Munkres matching cost (identical to the structured-only baseline; see Appendix G). Profile features add only the $O(|C| \cdot d)$ feature-concat term, which empirically contributes well under 1 ms per cycle (Appendix M).

(N3) Cold-start. Users without sufficient history are mapped to a default cluster at registration ($O(1)$); no additional online cost.

N.3 Storage Complexity

ProfiLLM's serving state comprises three components. The cluster embeddings occupy $|\mathcal{A}| \cdot d \cdot 4\,\mathrm{B} = 96 \times 768 \times 4 \approx 295\,\mathrm{KB}$; the user-to-cluster table stores a 32-bit cluster ID per user at 4 B each, $\approx 1.4\,\mathrm{MB}$ for the 348,464 users in City A; and the LOGIC rules and PROFILE text amount to $|\mathcal{A}|$ short strings, $\approx$ 50 KB. The active footprint is therefore a few MB per city, nearly three orders of magnitude smaller than caching a per-user d-dimensional embedding ($\approx$1 GB for City A).

N.4 Comparison with Per-User Profiling

Cluster-level profiling reduces both LLM-call count and embedding storage by a factor of $(M + N)/|\mathcal{A}|$. For City A:

$$\frac{|\mathcal{P} \cup \mathcal{D}|}{|\mathcal{A}|} = \frac{348{,}464}{96} \approx 3{,}630\times .$$

(The deployment registry contains 348,464 users; Appendix A reports 345,294 users active within a narrower 38-day analysis window, hence the small discrepancy.) This is the structural source of ProfiLLM's offline cost efficiency, and Appendix J confirms that this reduction does not sacrifice prediction quality once $|\mathcal{A}| > 16$.

N.5 Summary

Table 7 consolidates the analysis. Offline complexity is linear in data ($|\mathcal{H}|$) for tool execution and cluster assignment, and the LLM-call count is linear in the *cluster* count $|\mathcal{A}|$ rather than the *user* count $(M + N)$. Online complexity is dominated by the existing bipartite-matching solver; profile features add only $O(|C| \cdot d)$ FLOPs and two $O(1)$ cache lookups per OD pair. Storage for LLM-introduced artifacts is sub-MB.

Stage	Time	Notes
Knowledge Mining (O1)	$O(\lvert\mathcal{T}\rvert \cdot \lvert\mathcal{H}\rvert)$	$+\,O(1)$ LLM calls
Cluster Assignment (O2)	$O(\lvert\mathcal{A}\rvert \cdot \lvert\mathcal{H}\rvert)$	parallel
Profile Exploration (O3)	$O(K(1+T) \cdot \lvert\mathcal{H}\rvert)$	$+\,O(\lvert\mathcal{A}\rvert \cdot K(1+T))$ LLM calls
DPO Training (O4)	$O(E \cdot \lvert\mathcal{P}_{pref}\rvert \cdot L)$	one-time
Embedding (O5)	$O(\lvert\mathcal{A}\rvert \cdot L)$	seconds
Online per OD pair (N1)	$O(d + c_f)$	two cache lookups
Online per cycle (N2)	$O(\lvert C\rvert \cdot d) + O_{\mathrm{KM}}$	KM dominates
Embeddings storage	$O(\lvert\mathcal{A}\rvert \cdot d)$	$\approx$ 295 KB
User-cluster table	$O(M + N)$	$\approx$ 1.4 MB (City A)

Table 7: Complexity summary. $|\mathcal{H}|$: total history records; $|\mathcal{A}|$: cluster count; K=5, T=3; $|C|$: candidate OD pairs per cycle; d=768; c_f: constant prediction-network forward cost.

O EXTENDED 14-DAY A/B TEST: LONG-TERM STABILITY

The 14-day deployment in Section 4.5 extends the initial 5-day pilot to a longer window for more stable estimates. We summarize the comparison and broader generalization evidence here.

Stability over time. GMV improvement *grew* from +0.36% (5 days) to **+0.47%** (14 days) and CR rose from +0.16% to +0.33%, while every cancellation and bad-experience metric remained directionally negative across the full window (CBA, PCR, DCR, BER). The fact that effect sizes did not decay, and in several cases grew, over the extended observation period supports the interpretation that ProfiLLM produces durable matching-quality gains rather than transient effects.

Joint movement across funnel stages. Every monitored realized rate moves in the beneficial direction across mechanistically distinct stages of the fulfillment funnel: revenue/completion (GMV, CR), pre-acceptance attrition (CBA), post-acceptance cancellation (PCR, DCR), and completed-order experience (BER). Each stage reflects a different behavioral mechanism, so the joint consistency provides converging evidence that the improvement is systematic. A model that improves only one stage would be expected to show mixed signs elsewhere; the uniform direction here is consistent with profiling improving the underlying outcome prediction that feeds every stage.

Generalization beyond a single city. While the A/B was conducted in City A, the offline simulator evaluation in Table 1 covers three cities with distinct supply-demand regimes (City A supply-constrained, City B supply-relaxed, City C large-scale high-demand) and uses the production routing API for realistic ETA. ProfiLLM dominates baselines across all three cities and all time-of-day buckets (Figure 11), supporting that the online gains would carry over. Broader online rollout across additional cities is in progress and will be reported in a follow-up.

P PRIVACY AND FAIRNESS CONSIDERATIONS

Because user profiles directly influence which drivers receive which orders, we discuss the privacy and fairness implications of ProfiLLM explicitly.

Privacy by architectural design. Two safeguards limit exposure of individual data. (1) *Cluster-level abstraction.* The LLM never sees a single user's identifiable trajectory in isolation. It processes only cluster-pooled, re-sampled order records together with summary statistics aggregated over all members of a cluster (e.g., "this cluster of drivers cancels orders with pickup distance > 5 km during evening hours at rate r"). An individual user's data only contributes to a cluster's aggregate and cannot be reconstructed from the profile description. (2) *Offline-only LLM inference.* Every LLM call happens in the offline knowledge-mining and profile-exploration stages.

At serving time the online system performs only a deterministic cluster-assignment rule evaluation and a cache lookup for precomputed embeddings (Section 3.4); no user data is transmitted to any LLM API during real-time dispatching.

Driver earning equity. If certain driver clusters are profiled as "likely to cancel long-pickup orders," the system may avoid such assignments, improving platform efficiency but potentially affecting those drivers' earning opportunities. This is, however, the behavior any accurate prediction model would produce, whether using profiles or structured features; ProfiLLM merely makes the prediction signal more explicit and *auditable*. Platform operators can inspect the textual PROFILE of each cluster (Section 3.3.2) and verify it does not encode undesirable biases, a transparency advantage over opaque deep-feature interactions.

Passenger service equity. Infrequent users, including the 96% long-tail passengers in Figure 2, are still assigned to behavioral clusters via $a^*(u)$ and receive shared cluster-level profiles rather than being excluded from profiling (Section 3.4.2); only genuine cold-start users with no usable history fall back to a default cluster. They therefore receive at least baseline matching quality, closing the cold-start gap that per-user profiling methods would face.

Behavioral vs. protected attributes. The clustering rules use only behavioral features (order patterns, cancellation history, temporal activity, spatial preferences), never protected attributes. We acknowledge that behavioral features may correlate with such attributes (commute-hour patterns with occupation, frequent regions with socioeconomic status). The cluster-level design supports a tractable auditing path: outcome distributions (driver income, passenger wait time, allocation rates) can be measured across clusters and clusters with statistically anomalous treatment flagged. We are integrating such auditing into our deployment pipeline as an ongoing direction.

Q PROMPT TEMPLATE

We present the abstracted prompt template in Table 8.

Table 8: Prompt templates used for profile exploration. Placeholders denote injected inputs; the concrete feature legend and data tables are omitted.

Template	Abstracted Prompt
Driver—Draft	[Role] Expert analyst (data science + behavioral economics) for ride-hailing driver behavior. [Task] Infer a stable driver persona and decision logic. [Inputs] Summary: {SUMMARY_STATS}; Grouped recent records: {RECENT_GROUPED_RECORDS}. [Guidelines] Records may be re-sampled; focus on feature differences across outcomes; use only features in the provided legend. [Reasoning] (1) rejection patterns (ignored) (2) regret patterns (post-accept cancellations) (3) persona + generalizable rules. [Output] XML only: <ANALYSIS>, <PROFILE>, <LOGIC_ACCEPT> (1-line Python), <LOGIC_CANCEL> (1-line Python).
Driver—Improve	[Inputs] {SUMMARY_STATS}, {RECENT_GROUPED_RECORDS}, plus previous response {PREVIOUS_RESPONSE} and feedback {FEEDBACK}. [Task] Improve profile + logic to increase validation performance; change only what is justified by patterns and feedback. [Output] A complete, self-contained updated response (not a patch), in the same XML-only format.
Passenger—Draft	[Role] Expert analyst for ride-hailing passenger post-match behavior. [Task] Infer patience and post-match cancellation triggers. [Inputs] Summary: {SUMMARY_STATS}; Grouped recent records (completed vs cancelled-after-match): {RECENT_GROUPED_RECORDS}. [Guidelines] Compare feature differences across outcomes; use only features in the provided legend (high-level: price/trip, ETA/waiting, context such as time and weather). [Reasoning] (1) time vs money (2) sunk cost (3) context modifiers (4) persona synthesis. [Output] XML only: <ANALYSIS>, <PROFILE>, <LOGIC_CANCEL> (1-line Python).
Passenger—Improve	[Inputs] {SUMMARY_STATS}, {RECENT_GROUPED_RECORDS}, plus previous response {PREVIOUS_RESPONSE} and feedback {FEEDBACK}. [Task] Improve profile + logic with minimal, data-justified changes. [Output] A complete, self-contained updated response (not a patch), in the same XML-only format.